Available online at www.sciencedirect.com
ScienceDirect
Journal of Sound and Vibration 314 (2008) 330–342
JOURNAL OF SOUND AND VIBRATION
www.elsevier.com/locate/jsvi

A study on free vibration of a ring-stiffened thin circular cylindrical shell with arbitrary boundary conditions

Zhi Pan*, Xuebin Li, Janjun Ma

Wuhan 2nd Ship Design & Research Institute, Hubei Province, PR China

Received 1 July 2007; received in revised form 18 December 2007; accepted 4 January 2008
Handling Editor: L.G. Tham
Available online 4 March 2008

Abstract

The vibration of ring-stiffened cylinders associated with arbitrary boundary conditions is investigated. Displacements of cylinders can be easily described by trigonometric functions when the cylinders are shear diaphragms supported at both ends. As to other boundary conditions, exponential functions are used and axial factors are introduced. An eighth-order algebraic equation for this axial factor is derived. The physical meaning of the axial factor is studied. Both analytical and numerical studies prove that, when the axial factor is a pure imaginary number, the cylinder appears to have a certain length with shear diaphragm boundary conditions. The effects of shell parameters and hydrostatic pressure on the axial factor are determined in the analysis.

1. Introduction

The use of cylindrical shells is common in many fields, such as aerospace, mechanical, civil and marine engineering structures. To effectively enhance the flexural and axial stiffness, stiffeners are frequently used. Many engineers have considerable interest in the free vibration of thin circular cylindrical shells and numerous investigations have been devoted to this, e.g. Ref. [1–6]. The methods used to study the vibrational behavior of thin shells range from energy methods based on the Rayleigh–Ritz procedure to analytical methods in which, respectively, closed–form solutions of the governing equations and iterative solution approaches were used. The circular cylindrical shell supported at both ends by shear diaphragms (SD–SD) has received the most attention in the literatures. This is due to the fact that one simple form of the solutions to the eighth-order differential equations of motion is capable of satisfying the SD–SD boundary conditions exactly. The frequency equation is a polynomial of order six in the shell frequency parameter. When solving problems with arbitrary boundary conditions, many authors [7–11] select general solutions of shell equations. They have chosen exponential functions for the modal displacements along the axial direction, substituted them into the equations of motion and then enforced the eighth-order frequency determinants which are coupled together.

*Corresponding author.
E-mail address: pan_zhi@yahoo.com.cn (Z. Pan).

0022-460X/$ - see front matter © 2008 Elsevier Ltd. All rights reserved.
doi:10.1016/j.jsv.2008.01.008

Nomenclature

A_2	sectional area of the stiffener
B	stretching stiffness of the shell, $B = Eh/1-\mu^2$
b_r	width of the rectangular stiffener
D	bending stiffness of the shell, $D = Eh^3/12(1-\mu^2)$
d_2	stiffener spacing
E	modulus of Young's elasticity
e_2	eccentricity of the centroid of the ring stiffener section
G	shear modulus
h	thickness of the shell
$\overline{h}$	$h+A_2/d_2$
h_r	height of the rectangular stiffener
I_0	sectional moment of inertia of the stiffener about the centroid of the stiffener
I_2	sectional moment of inertia of the stiffener about the middle surface of the shell
i	$\sqrt{-1}$
J_2	torsion constant of stiffener cross-section
k	$h^2/12R^2$
L	length of the shell between ends
m	axial mode number
n	number of circumferential waves
Q	hydrostatic pressure
R	radius of the mean surface of the shell
t	time
x, θ, z	cylindrical coordinates (Fig. 1)
U_n, V_n, W_n	amplitudes of the displacement in the x, θ and z directions
u, v, w	components of the displacement in the x, θ and z directions
λ	axial factor
μ	Poisson's ratio
ρ	mass density
ω	circular frequency

Recently, many new approaches were developed for cylinder shell for free vibration analysis of cylindrical and conical shells. Xiang et al. [12] use the state-space technique to derive the homogenous differential equation system for a shell segment and a domain decomposition approach is developed to cater to the continuity requirements between shell segments. Bingen Yang and Jianping Zhout [13] have used the distributed transfer functions of the structural components, and then various static and dynamic problems of stiffened shells have been systematically formulated. With this transfer function formulation, the static and dynamic response, natural frequencies and mode shapes and buckling loads of general stiffened cylindrical shells under arbitrary external excitations and boundary conditions can be determined in exact and closed forms. Civalek Ömer [14] proposes a discrete singular convolution method for the free vibration analysis of rotating conical shells. Frequency parameters of the forward modes are obtained for different types of boundary conditions, rotating velocity and geometric parameters. A wave propagation approach [15–18] is also developed to predict the natural frequency of the cylinders. This method combines an exact frequency wavenumber characteristic formula with appropriate beam functions in the axial direction to give predictions of natural frequencies of circular cylindrical shells.

In the general solutions of shell equations, axial factors are usually introduced. But few literatures have discussed the physical meanings of the axial factors. It has been numerically proved that the modes associated with pure imaginary axial factors conform to the shear diaphragm end conditions of a finite shell of length [19]. The analysis in this paper complements the author's previous work [19] in the sense that it investigates the physical meaning of the axial factors both numerically and analytically, and the effects of the shells' parameters and hydrostatic pressure are also studied. In this paper, a general solution using exponential functions for the modal displacements along both the axial and the circumferential directions is presented.

The investigation into the problem of the cylinder stiffened by ring stiffeners uses a "smeared frame" approach, and represents the discretely reinforced cylinder by a uniformly orthotropic cylinder. When the stiffener spacing increases or becomes irregular or if the wavelength of the eigenmode becomes smaller than the stiffener spacing, this approach is no longer useful. The classical linear shell theory of Flügge [3] is adopted in the present analysis.

2. Exact solution of motion equations

The stiffeners are not considered as discrete members, but their effects are averaged or "smeared out" over the shell. Shell equations of motion for a thin-walled circular cylinder, stiffened by evenly spaced uniform rings (Fig. 1) under hydrostatic pressure, are given below according to Flügge's shell theory:

$$\begin{aligned}
&\frac{\partial N_x}{\partial x}+\frac{\partial N_{\theta x}}{R\partial\theta}-Q\left(\frac{\partial^2 u}{R\partial\theta^2}+\frac{\partial w}{\partial x}\right)-\frac{QR}{2}\frac{\partial^2 u}{\partial x^2}=\rho\bar{h}\frac{\partial^2 u}{\partial t^2},\\
&\frac{\partial N_{x\theta}}{\partial x}+\frac{\partial N_\theta}{R\partial\theta}-\frac{1}{R}\left(\frac{\partial M_\theta}{R\partial\theta}+\frac{\partial M_{x\theta}}{\partial x}\right)-Q\left(\frac{\partial^2 v}{R\partial\theta^2}-\frac{\partial w}{R\partial\theta}\right)-\frac{QR}{2}\frac{\partial^2 v}{\partial x^2}=\rho\bar{h}\frac{\partial^2 v}{\partial t^2},\\
&\frac{\partial^2 M_x}{\partial x^2}+\frac{\partial^2 M_{x\theta}}{R\partial x\partial\theta}+\frac{\partial^2 M_{\theta x}}{R\partial x\partial\theta}+\frac{\partial^2 M_\theta}{R^2\partial\theta^2}+\frac{N_\theta}{R}+Q\left(\frac{\partial u}{\partial x}-\frac{\partial v}{R\partial\theta}-\frac{\partial^2 w}{R\partial\theta^2}\right)-\frac{QR}{2}\left(\frac{\partial^2 w}{\partial x^2}\right)=\rho\bar{h}\frac{\partial^2 w}{\partial t^2}.
\end{aligned}\tag{1}$$

The forces and moments are given in the Appendix.

The general solution for the equations can be written in the following form:

$$(u_n(x,\theta),\ v_n(x,\theta),\ w_n(x,\theta))=(U_n,\ V_n,\ W_n)\mathrm{e}^{\lambda x/R}e^{\mathrm{i}n\theta}\mathrm{e}^{\mathrm{i}\omega t},\tag{2}$$

where the axial factor λ is a complex number.

Substituting Eq. (2) into Eq. (1), it can be written as

$$[L_{jk}]\{U_n,\ V_n,\ W_n\}^{\mathrm{T}}=\{0\};\quad j,\ k=1,\ 2,\ 3.\tag{3}$$

The elements of the coefficient matrix L_{jk} are given in the Appendix.

The nondimensional circular frequency and hydrostatic pressure used in Eq. (3) are given as

$$\Omega^2=\frac{\rho(1-\mu^2)R^2}{E}\omega^2,\tag{4}$$

$$Q'=\frac{QR(1-\mu^2)}{Eh}.\tag{5}$$

For the unstiffened cylinder case, the coefficient matrix of Eq. (3) is symmetrical. The coefficient matrix that contains the influence of hydrostatic pressure is always antisymmetric.

For nontrivial solutions of Eq. (3), one requires

$$\det(L_{jk})=0;\quad j,k=1,\ 2,\ 3.\tag{6}$$

The determinant can be expressed as

$$F(\omega,\ n,\ \lambda,\ Q')=0.\tag{7}$$

Assuming a known vibration frequency and a number of circumferential waves n, we can obtain an eighth-order algebraic equation for λ:

$$P_8\lambda^8+P_6\lambda^6+P_4\lambda^4+P_2\lambda^2+P_0=0.\tag{8}$$

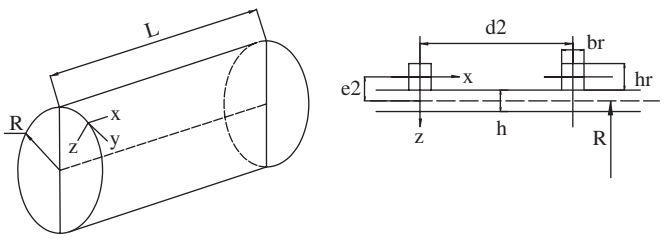

Fig. 1. Ring-stiffened circular cylindrical shell.

The roots of Eq. (8) usually have the form [6]:

$$\lambda = \pm k_1 \pm \mathrm{i}k_2, \quad \pm k_3, \pm \mathrm{i}k_4 \tag{9}$$

where k_j ($j = 1, 2, 3, 4$) are real quantities.

Analytical solutions for Eq. (8) can be written as

$$\begin{aligned}
(\lambda_{1,2})^2 &= \Gamma_{16} - \frac{\sqrt{\Lambda_1}}{2} - \frac{1}{2}\sqrt{\Lambda_2 - \frac{\Lambda_3}{4\sqrt{\Lambda_1}}};\\
(\lambda_{3,4})^2 &= \Gamma_{16} - \frac{\sqrt{\Lambda_1}}{2} + \frac{1}{2}\sqrt{\Lambda_2 - \frac{\Lambda_3}{4\sqrt{\Lambda_1}}},\\
(\lambda_{5,6})^2 &= \Gamma_{16} + \frac{\sqrt{\Lambda_1}}{2} - \frac{1}{2}\sqrt{\Lambda_2 + \frac{\Lambda_3}{4\sqrt{\Lambda_1}}};\\
(\lambda_{7,8})^2 &= \Gamma_{16} + \frac{\sqrt{\Lambda_1}}{2} + \frac{1}{2}\sqrt{\Lambda_2 + \frac{\Lambda_3}{4\sqrt{\Lambda_1}}},
\end{aligned} \tag{10}$$

where

$$\begin{aligned}
&\Gamma_1 = P_4^2 - 3P_2P_6 + 12P_0P_8,\\
&\Gamma_2 = 2P_4^3 - 9P_2P_4P_6 + 27P_0P_6^2 + 27P_2^2P_8 - 72P_0P_4P_8,\\
&\Gamma_3 = (-4\Gamma_1^3 + \Gamma_2^2)^{1/2}, \quad \Gamma_4 = \Gamma_2 + \Gamma_3,\\
&\Gamma_5 = \Gamma_4^{1/3}, \quad \Gamma_6 = 2^{1/3}\Gamma_1,\\
&\Gamma_7 = P_6^2/4P_8^2, \quad \Gamma_8 = \Gamma_5/3P_8 2^{1/3},\\
&\Gamma_9 = \Gamma_6/3\Gamma_4^{1/3}P_8, \quad \Gamma_{10} = -8P_2/P_8,\\
&\Gamma_{11} = P_6^3/P_8^3, \quad \Gamma_{12} = 4P_4P_6/P_8^2,\\
&\Gamma_{13} = -2P_4/3P_8, \quad \Gamma_{14} = P_6^2/2P_8^2,\\
&\Gamma_{15} = -1/3P_8 2^{1/3}, \quad \Gamma_{16} = -P_6/4P_8,\\
&\Gamma_{17} = -4P_4/3P_8, \quad \Gamma_{18} = -\Gamma_6/3\Gamma_4^{1/3}P_8,\\
&\Lambda_1 = \Gamma_{13} + \Gamma_7 + \Gamma_8 + \Gamma_9, \quad \Lambda_2 = \Gamma_{14} + \Gamma_{17} + \Gamma_{18} + \Gamma_{15}\Gamma_5,\\
&\Lambda_3 = \Gamma_{10} - \Gamma_{11} + \Gamma_{12}.
\end{aligned}$$

3. Numerical examples

An examples is studied in the present analysis. The assumptions for the basic parameters of shells and stiffeners are [20]: $h = 0.119 \times 10^{-2}$ m, $R = 10.37 \times 10^{-2}$ m, $d_2 = 3.14 \times 10^{-2}$ m, $b_r = 0.218 \times 10^{-2}$ m, $h_r = 0.291 \times 10^{-2}$ m, and $\mu = 0.3$, $E = 2.06 \times 10^{11}$ N/m^2.

The roots of Eq. (8) are computed for the following five cases:

(1) an unstiffened shell with Ω variation for $Q' = 0$ and $n = 3$.
(2) an unstiffened shell with Ω variation for $Q' = 0$ and $n = 9$.
(3) an internal-ring stiffened shell with Ω variation for $Q' = 0.008$ and $n = 3$.
(4) an unstiffened shell with Ω variation for $Q' = 0.008$ and $n = 9$.
(5) an internal-ring stiffened shell with Ω variation for $Q' = 0.008$ and $n = 9$.

The results from Eq. (10) are shown in Figs. 2–6 for nondimensional frequencies. At any frequency, four distinctly different values of λ are seen to exist, although only two may be seen on the figures. This is due to

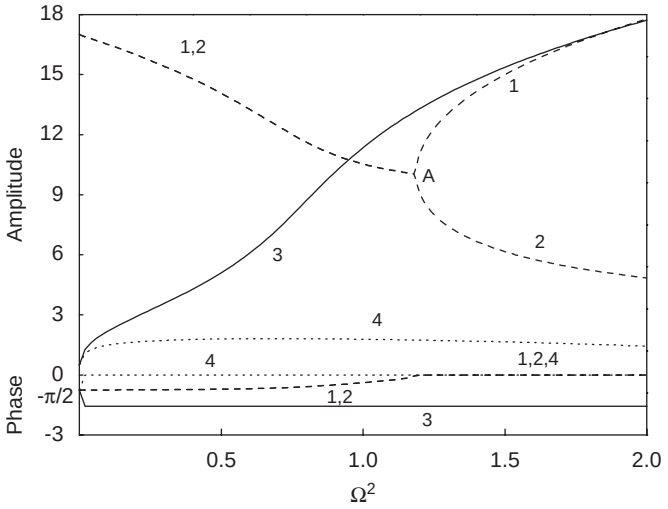

Fig. 2. Roots of Eq. (8) for unstiffened cylinders ($n = 3$, $Q = 0$).

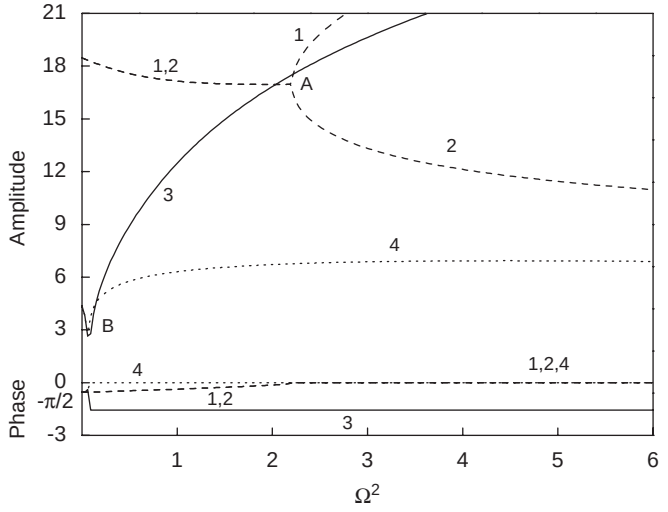

Fig. 3. Roots of Eq. (8) for unstiffened cylinders ($n = 9$, $Q = 0$).

curves 1, 2 and 3, 4 representing coincident complex conjugate pairs. Each curve has its negative counterpart, meaning that eight λ exist altogether at any frequency. The phrases are $-\pi/2$ and 0 indicate that λ is pure imaginary or real, respectively.

It can be seen in the figures that curves 1 and 2 always translate to two curves representing pure real roots at point A from coincident complex conjugate pairs. Curves 3 and 4 always represent pure imaginary roots and real roots, respectively, over the frequency ranges calculated, except in Fig. 3. Fig. 3 shows that curves 3 and 4 represent coincident complex conjugate pairs in the very low frequency range, and translate to curves 3 and 4 at point B.

A further comparison made between Figs. 3 and 5 shows that hydrostatic pressure delays the appearance of bifucation point A, and increases the amplitude of the pure imaginary roots markedly. Hydrostatic pressure does not effect curves 1, 2, 4 very much. Examination of Figs. 2 and 3 shows that point A appears much later in high-order vibration than in low-order vibration. The stiffeners affect mainly the initial values of the pure imaginary roots on comparing Fig. 5 with 6.

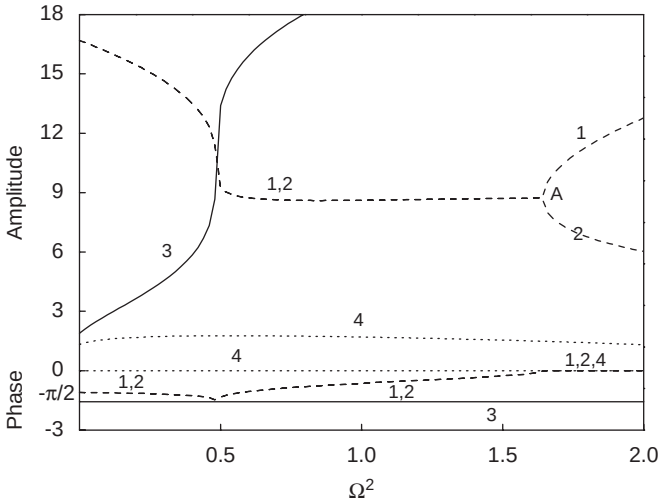

Fig. 4. Roots of Eq. (8) for internal-ring cylinders ($n = 3$, $Q' = 0.008$).

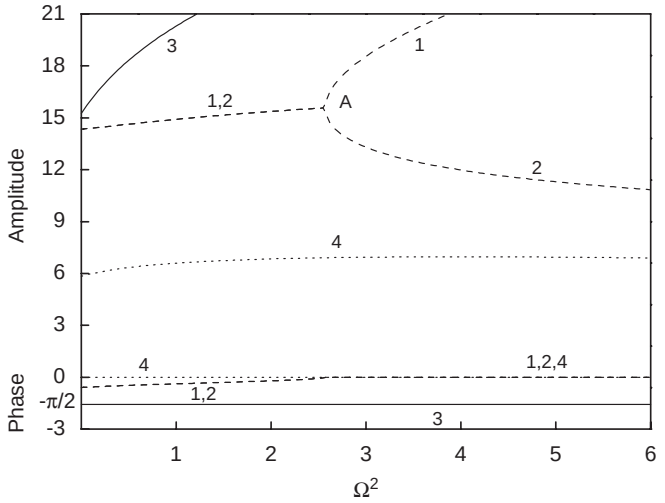

Fig. 5. Roots of Eq. (8) for unstiffened cylinders ($n = 9$, $Q' = 0.008$).

3.1. The physical meaning of pure imaginary roots

The above calculations show that Eq. (8) has the pure imaginary roots as $\pm i\lambda_s$ for certain combinations of (ω, n, Q'). Substituting $\lambda = \pm i\lambda_s$ into Eq. (8), Eq. (8) can be rewritten as

$$P_8\lambda_s^8 - P_6\lambda_s^6 + P_4\lambda_s^4 - P_2\lambda_s^2 + P_0 = 0. \tag{11}$$

In order to investigate the physical meaning of the pure imaginary roots, the classical separation of variables, method for determining the natural frequencies of cylinders with shear diaphragm boundary conditions is deduced here. A comparison will be made between two approaches. Suppose that the cylinders supported at both ends by shear diaphragms (SD–SD) have a certain length L for classical analysis. The shear diaphragm boundary conditions can be closely approximated in physical application simply by means of rigidly attaching a thin, flat, circular cover plate at each end [6].

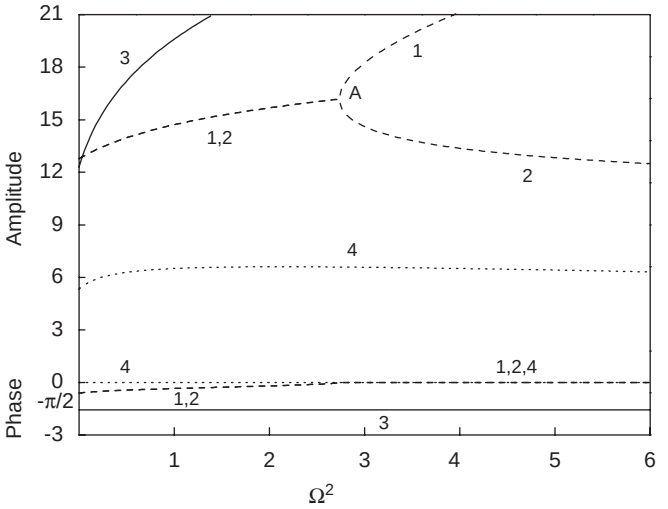

Fig. 6. Roots of Eq. (8) for internal-ring cylinders ($n = 9$, $Q' = 0.008$).

Consider the closed circular cylindrical shell of finite length L which satisfies the boundary conditions

$$v = w = N_x = M_x = 0 \quad \text{at ends.} \tag{12}$$

Generally, deformation functions for the boundary conditions are given as follows:

$$\begin{aligned} u_{mn}(x,\theta) &= U_{mn}\cos(n\theta)\cos(\lambda_{\mathrm{cl}}x)\cos\omega_{\mathrm{cl}}t, \\ v_{mn}(x,\theta) &= V_{mn}\sin(n\theta)\sin(\lambda_{\mathrm{cl}}x)\cos\omega_{\mathrm{cl}}t, \\ w_{mn}(x,\theta) &= W_{mn}\cos(n\theta)\sin(\lambda_{\mathrm{cl}}x)\cos\omega_{\mathrm{cl}}t, \end{aligned} \tag{13}$$

where $\lambda_{\mathrm{cl}} = m\pi R/L$.

Substituting Eq. (13) into Eq. (1), a set of equations similar to Eq. (3) is obtained. For nontrivial solution of equations, the determinant of the coefficient matrix must be zero. This leads to an equation with variables $(\omega_{\mathrm{cl}}, m, n, \lambda_{\mathrm{cl}}, Q'_{\mathrm{cl}})$ as follows:

$$F_2\left(\omega_{\mathrm{cl}}, m, n, \lambda_{\mathrm{cl}}, Q'_{\mathrm{cl}}\right) = 0. \tag{14}$$

Eq. (14) is a cubic equation with variable vibration frequency ω_{cl}^2 when $\lambda_{\mathrm{cl}} = m\pi R/L$ is given. Each combination of m and n has three roots of frequency. The minimum root among the roots for all combinations of m and n is namely the basic frequency of the cylinder.

Eq. (14) can also be written as an eighth-order algebraic equation for λ_{cl}:

$$P'_8\lambda_{\mathrm{cl}}^8 + P'_6\lambda_{\mathrm{cl}}^6 + P'_4\lambda_{\mathrm{cl}}^4 + P'_2\lambda_{\mathrm{cl}}^2 + P'_0 = 0. \tag{15}$$

A comparison was made between $\{P_8, P_6, P_4, P_2, P_0\}$ and $\left\{P'_8, P'_6, P'_4, P'_2, P'_0\right\}$; it is interesting to note that:

$$P'_8 = P_8, \quad P'_6 = -P_6, \quad P'_4 = P_4, \quad P'_2 = P_2, \quad P'_0 = P_0. \tag{16}$$

These findings appear to prove that Eqs. (11) and (15) are the same. This reasoning certainly seems to offer a mathematical explanation for the conclusion that, when the axial factor is a pure imaginary number, the general solution, Eq. (2), for the shell equations appears to describe the vibration mode of a cylinder with a certain length and shear diaphragm boundary conditions. The length of the cylinder can be obtained from

$$|\lambda_s| = \frac{m\pi R}{L}. \tag{17}$$

After a pure imaginary root is obtained from Eq. (8), the length (L/R) of the cylinder with shear diaphragms supported at ends is determined according to Eq. (17). Then the, corresponding natural frequency ω_{cl} from Eq. (14) is compared with the given frequency ω, which is given before Eq. (8), and is resolved. Incidentally,

if the cylinder is shear diaphragm supported, the length of the cylinder equals to m multiplies the half-wavelength in the axial direction; hence, only $m = 1$ is discussed in the paper.

A numerical example is given for comparison in Table 1. Good agreement can be seen between the approach presented and the classical method for cylinders with shear diaphragm boundary conditions on comparing the second column with the fifth column.

3.2. Effects of Stiffeners on λ_s

The effects of stiffeners on pure imaginary roots are studied here. The symmetrical-ring stiffened cylinder is introduced here to make a comparison. The eccentricity of the centroid of ring stiffener section e_2 equals to zero when the ring is symmetrical.

Fig. 7 shows that the values of $|\lambda_s|$ increase along with an increase of frequency. The starting points of the pure imaginary roots in Fig. 7 are the bifurcation points of the complex conjugate pairs. In order to compare the difference of the curves in Fig. 7 clearly, curves of differences based on internal-ring cylinder are shown in Fig. 8. The difference is defined as

$$\mathrm{Diff}_{\lambda}\left|\frac{|\lambda_s^{2,3}| - |\lambda_s^{1}|}{\lambda_s^{1}}\right| \times 100\%, \tag{18}$$

Table 1
Comparison with classical method

Present approach (Eq. (7))		Classical method (Eq. (14))	
Ω	$\lvert\lambda_s\rvert$	$L_{\mathrm{cl}}(\times 10^{-2})$	Ω_{cl}
$n = 3$			
0.1	1.0362	31.44018	0.10000
0.5	3.2444	10.04137	0.50000
1.0	11.3558	2.86886	1.00000
1.5	18.6236	1.75129	1.49792

Unstiffened shell, $Q' = 0$, $h = 0.119 \times 10^{-2}$ m, $R = 10.37 \times 10^{-2}$ m, $E = 2.06 \times 10^{11}$ N/m^2, $\mu = 0.3$.

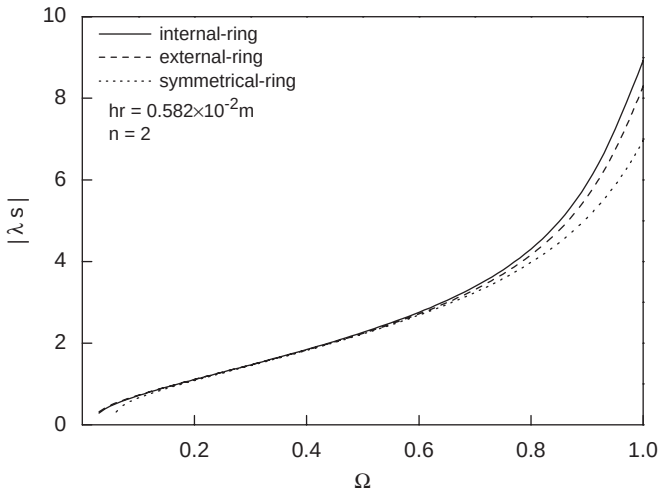

Fig. 7. Effects of stiffeners' locations ($Q = 0$).

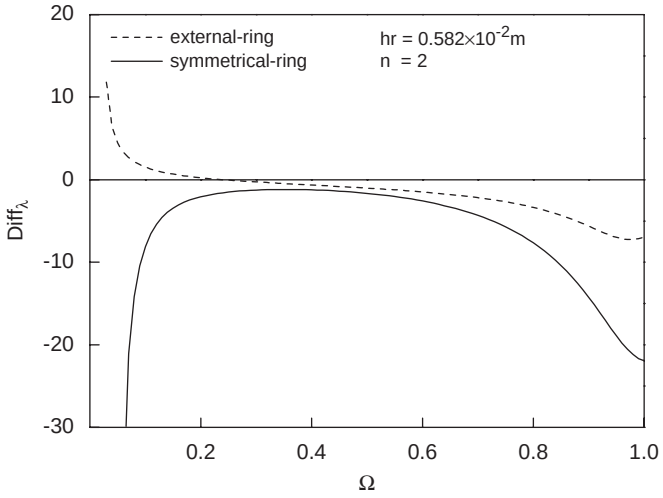

Fig. 8. Curves of difference in stiffeners' locations.

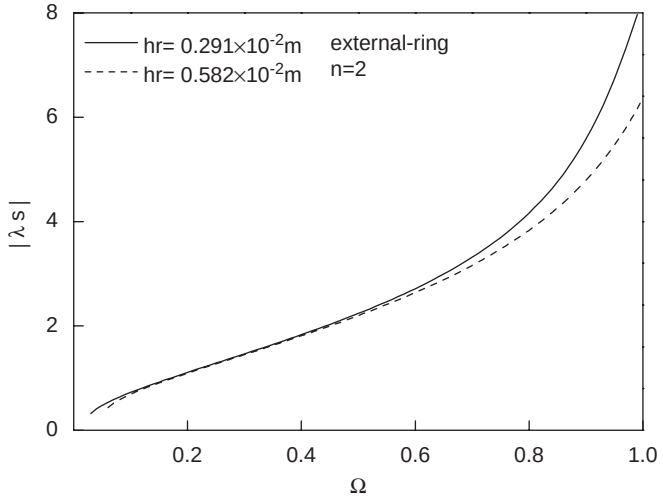

Fig. 9. Effects of stiffeners' parameters ($Q = 0$).

where λ_s^1 corresponds to the internal ring; $\lambda_s^{2,3}$ corresponds to the external ring and the symmetrical ring, respectively.

It can be seen in Fig. 8 that $|\lambda_s|$ obtained from the external-ring cylinder are greater than those obtained from the internal-ring cylinder when $\Omega < 0.235$, but smaller when $\Omega > 0.235$. $|\lambda_s|$ obtained from the symmetrical-ring cylinder are always the smallest in the frequency ranges. This indicates that the natural frequency of the symmetrical-ring cylinder is always the highest in the three location forms.

The effects on $|\lambda_s|$ of stiffeners' parameters with no initial pressure($Q' = 0$) are shown in Fig. 9. It can be seen that the stronger the ring, the smaller the $|\lambda_s|$, meaning that the increase of stiffeners' stiffness heightens the cylinder's natural frequency. Fig. 10 shows the difference between $|\lambda_s|$ obtained from the stiffeners of two different sizes, and the difference is defined as Eq. (18). It can be seen that the difference fluctuates from large to small along with a reduction in shell length.

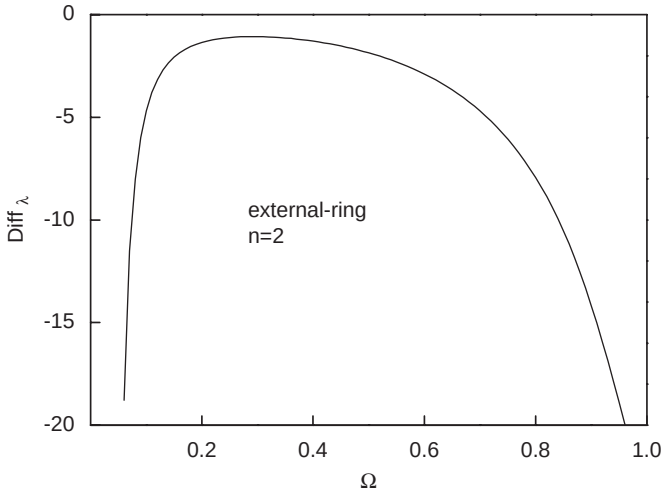

Fig. 10. Curves of difference in stiffeners' parameters.

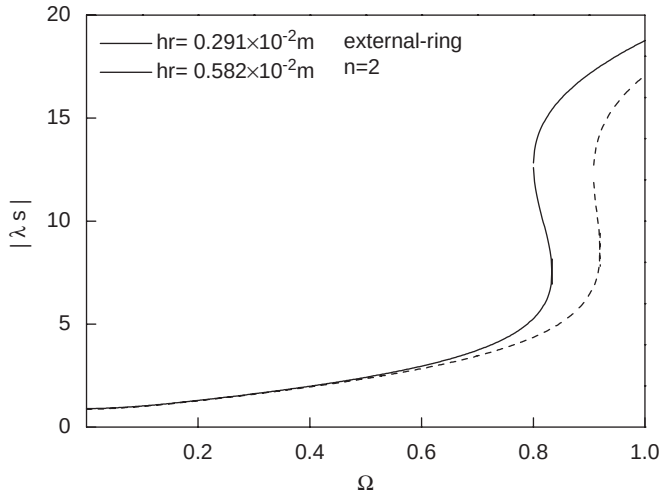

Fig. 11. Effects of stiffeners' parameters($Q' = 0.008$).

When the hydrostatic pressure exists($Q' = 0.008$), the effects of stiffeners' parameters are presented in Fig. 11. The hydrostatic pressure increases the value of $|\lambda_s|$, and the increase of stiffeners' stiffness increase the cylinder's natural frequency as we found with no hydrostatic pressure. As multiple values appear with increasing frequency, we cannot obtain the difference line between the two lines in the whole frequency range. Before multiple values appear, the hydrostatic pressure reduces the difference between the two lines in the low-frequency range, but heighten the difference in the high-frequency range.

3.3. *Effects of initial stress on λ_s*

In this paper, hydrostatic pressure is considered as the initial stress. Figs. 12 and 13 show the effects of hydrostatic pressure on the pure imaginary roots. It can be seen that hydrostatic pressure reduces the natural frequency of cylinders with a certain length. Hydrostatic pressure has much more effects on the vibration behavior when the vibration order is higher. Curves start at zero frequency, which

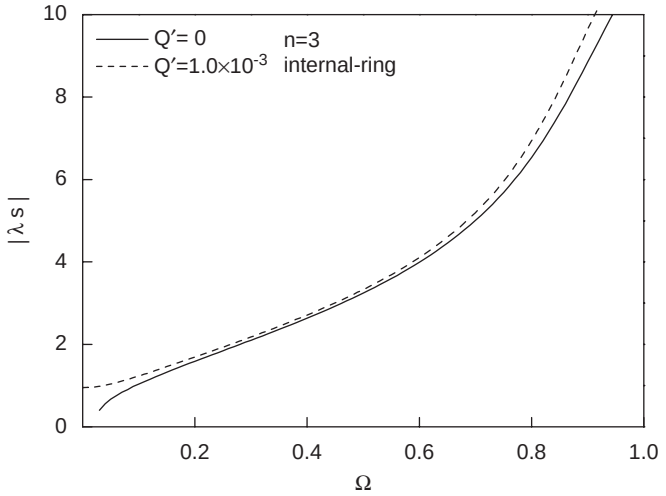

Fig. 12. Effects on high-order vibration of hydrostatic pressure ($n = 3$) (internal-ring, $b_r = 0.218 \times 10^{-2}$ m, $h_r = 0.291 \times 10^{-2}$ m).

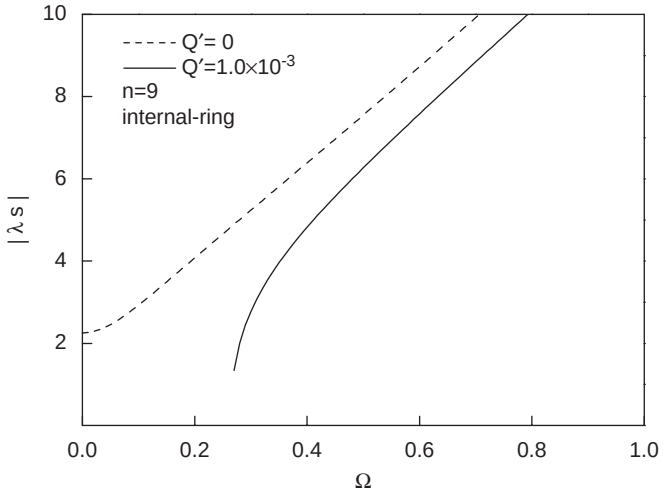

Fig. 13. Effects on low-order vibration of hydrostatic pressure ($n = 9$) (internal-ring, $b_r = 0.218 \times 10^{-2}$ m, $h_r = 0.291 \times 10^{-2}$ m).

indicates that the hydrostatic pressure is just the buckling pressure of the cylinder with shear diaphragm ends.

4. Conclusion

When solving the vibration problem of ring-stiffened cylinders associated with arbitrary boundary conditions, exponential functions are used and axial factors are introduced here. An eighth-order algebraic equation for this axial factor is derived. The physical meaning of the axial factor is studied. Both analytical and numerical researches prove that when the axial factor is a pure imaginary number, the cylinder appears to have a certain length with shear diaphragm boundary conditions. The effects of stiffeners' parameters and hydrostatic pressure on the axial factor are studied.

Hydrostatic pressure increases the module of the pure imaginary roots markedly, but does not affect the other curves very much. The stiffeners affect mainly the initial value of the pure imaginary roots. The natural

frequency of the symmetrical-ring stiffened cylinder is always the highest in the three disposal forms. Increasing the stiffeners' stiffness can increase the cylinder's natural frequency.

Appendix A. Forces and moments

Eight internal forces including membrane forces N_x, N_θ, $N_{x\theta}$ and $N_{\theta x}$, bending moments M_x and M_θ and torsioning moments $M_{x\theta}$ and $M_{\theta x}$ are given

$$
\begin{aligned}
N_x &= B\left[\frac{\partial u}{\partial x}+\mu\left(\frac{\partial v}{R\partial\theta}-\frac{w}{R}\right)\right]+\frac{D}{R}\frac{\partial^2 w}{\partial x^2},\\
N_\theta &= B\left[(1+\mu_2)\left(\frac{\partial v}{R\partial\theta}-\frac{w}{R}\right)+\mu\frac{\partial u}{\partial x}-\chi_2\left(\frac{w}{R}+\frac{\partial^2 w}{R\partial\theta^2}\right)\right]-\frac{D}{R}\left(\frac{\partial^2 w}{R^2\partial\theta^2}+\frac{w}{R^2}\right),\\
N_{\theta x} &= \frac{1-\mu}{2}B\left(\frac{\partial u}{R\partial\theta}+\frac{\partial v}{\partial x}\right)+\frac{(1-\mu)D}{2R}\left[\frac{\partial u}{R^2\partial\theta}-\frac{\partial^2 w}{R\partial x\partial\theta}\right],\\
N_{x\theta} &= \frac{1-\mu}{2}B\left(\frac{\partial u}{R\partial\theta}+\frac{\partial v}{\partial x}\right)+\frac{(1-\mu)D}{2R}\left[\frac{\partial^2 w}{R\partial x\partial\theta}+\frac{\partial v}{R\partial x}\right],\\
M_x &= D\left[-\frac{\partial^2 w}{\partial x^2}-\mu\frac{\partial^2 w}{R^2\partial\theta^2}-\frac{\partial u}{R\partial x}-\mu\frac{\partial v}{R^2\partial\theta}\right],\\
M_\theta &= D\left[-(1+\eta_2)\left(\frac{w}{R^2}+\frac{\partial^2 w}{R^2\partial\theta^2}\right)-\mu\frac{\partial^2 w}{\partial x^2}+\zeta_2\left(\frac{\partial v}{R^2\partial\theta}-\frac{w}{R^2}\right)\right],\\
M_{x\theta} &= (1-\mu)D\left(-\frac{\partial^2 w}{R\partial x\partial\theta}-\frac{\partial v}{R\partial x}\right),\\
M_{\theta x} &= D\left[(1-\mu)\left(-\frac{\partial^2 w}{R\partial x\partial\theta}+\frac{1}{2R}\left(\frac{\partial u}{R\partial\theta}-\frac{\partial v}{\partial x}\right)\right)-\eta_{t_2}\frac{\partial^2 w}{R\partial x\partial\theta}\right].
\end{aligned}
$$

Appendix B. The elements of the coefficient matrix

$$
\begin{aligned}
L_{11} &= \lambda^2+\frac{(1-\mu)}{2}(1+k)(\mathrm{i}n)^2-Q'\left((\mathrm{i}n)^2+\frac{\lambda^2}{2}\right)+\Omega^2,\\
L_{12} &= \frac{(1-\mu)}{2}\lambda\mathrm{i}n,\\
L_{13} &= -\lambda\mu+k\lambda^3-\frac{(1-\mu)k}{2}\lambda(\mathrm{i}n)^2-Q'\lambda,\\
L_{21} &= \frac{(1-\mu)}{2}\lambda\mathrm{i}n,\\
L_{22} &= (1+\mu_2)(\mathrm{i}n)^2-k\zeta_2(\mathrm{i}n)^2+\frac{1-\mu}{2}(1+3k)\lambda^2-Q'\left((\mathrm{i}n)^2+\frac{\lambda^2}{2}\right)+\Omega^2,\\
L_{23} &= -(1+\mu_2)\mathrm{i}n+\frac{(3-\mu)}{2}\lambda^2\mathrm{i}nk+\eta_2\left[\mathrm{i}n+(\mathrm{i}n)^3\right]k-\zeta_2(\mathrm{i}n)^3k+Q'(\mathrm{i}n),\\
L_{31} &= \lambda\mu-\lambda^3k+\frac{(1-\mu)}{2}\lambda(\mathrm{i}n)^2k+Q'\lambda,\\
L_{32} &= (1+\mu_2)\mathrm{i}n-\frac{(3-\mu)}{2}\lambda^2\mathrm{i}nk+\zeta_2(\mathrm{i}n)^3k-Q'\mathrm{i}n,\\
L_{33} &= k\left\{-\lambda^4-(2+\eta_{t_2})\lambda^2(\mathrm{i}n)^2-(1+\eta_2)(\mathrm{i}n)^4-(2+2\zeta_2+\eta_2)(\mathrm{i}n)^2-(1+\zeta_2)\right\}\\
&\quad -(1+\mu_2)-Q'\left((\mathrm{i}n)^2+\frac{\lambda^2}{2}\right)+\Omega^2,
\end{aligned}
$$

where

$$\mu_2 = \frac{EA_2}{Bd_2}, \quad \chi_2 = \frac{EA_2e_2}{Rd_2B}, \quad \eta_2 = \frac{EI_2}{Dd_2}, \quad \eta_{t_2} = \frac{GJ_2}{Dd_2}, \quad \zeta_2 = \frac{12R^2\chi_2}{h^2}.$$

References

[1] L. Rayleigh, *The Theory of Sound*, Dover Publications, New York, 1945.
[2] A.E.H. Love, *Mathematical Theory of Elasticity*, fourth ed, Dover, New York, 1944.
[3] W. Flügge, *Stress in Shell*, first ed, Springer, Berlin, 1934.
[4] R.N. Arnold, G.B. Warburton, Flexural vibrations of the walls of thin cylindrical shells having freely supported ends, *Proceedings of the Royal Society, A* 197 (1949) 238–256.
[5] R.N. Arnold, G.B. Warburton, The flexural vibrations of thin cylinders, *Proceedings of the Institution of Mechanical Engineers, A* 167 (1953) 62–80.
[6] A.W. Leissa, Vibration of Shells, NASA, SP-288, 1973.
[7] K. Forsberg, Influence of boundary conditions on the modal characteristics of thin cylindrical shells, *AIAA Journal* 2 (1964) 2150–2157.
[8] G.B. Warburton, J. Higgs, Natural frequencies of thin cantilever cylindrical shells, *Journal of Sound Vibration* 11 (3) (1970) 335–338.
[9] G.B. Warburton, Vibrations of thin circular cylindrical shell, *Journal of Mechanical Engineering Science* 7 (4) (1965) 399–407.
[10] R.L. Goldman, Mode shapes and frequencies of clamped–clamped cylindrical shells, *AIAA Journal* 12 (1974) 1755–1756.
[11] A. Ludwig, R. Krieg, An analytical quasi-exact method for calculating eigenvibraitons of thin circular cylindrical shells, *Journal of Sound and Vibration* 74 (2) (1981) 155–174.
[12] Y. Xiang, Y.F. Ma, S. Kitipornchai, C.W. Lim, C.W.H. Lau, Exact solutions for vibration of cylindrical shells with intermediate ring supports, *International Journal of Mechanical Sciences* 44 (2002) 1907–1924.
[13] B. Yang, J. Zhout, Analysis of ring-stiffened cylindrical shells, *Journal of Applied Mechanics* 62 (4) (1995) 1005–1014.
[14] C. Ömer, An efficient method for free vibration analysis of rotating truncated conical shells, *International Journal of Pressure Vessels and Piping* 83 (1) (2006) 1–12.
[15] C. Wang, J.C.S. Lai, Prediction of natural frequencies of finite length circular cylindrical shells, *Applied Acoustics* 59 (2000) 385–400.
[16] X.M. Zhang, G.R. Liu, K.Y. Lam, Vibration analysis of thin cylindrical shells using wave propagation approach, *Journal of Sound and Vibration* 239 (3) (2001) 397–403.
[17] C. Wang, J.C.S. Lai, Vibration analysis of finite length circular cylindrical shells with different boundary conditions, *Proceedings of Inter-noise 97*, Vol. 2, Budapest, Hungary, 1997, pp. 1561–1564.
[18] C. Wang, J.C.S. Lai, Comments on "Vibration analysis of thin cylindrical shell using the wave propagation approach," *Journal of Sound and Vibration* 249 (5) (2002) 1011–1015.
[19] X.B. Li, A new approach for free vibration analysis of thin circular cylindrical shell, *Journal of Sound and Vibration* 296 (2006) 91–98.
[20] N.L. Basdekas, M. Chi, Response of oddly-stiffened circular cylindrical shell, *Journal of Sound and Vibration* 17 (2) (1971) 187–206.